Chapter-5

Methyl-orange disintegration by MgZnAl-CO_3 layered double hydroxide (LDH) and its derivatives

5.1. Abstract

In this study, both uncalcined and calcined $[Mg_{0.5}^{2+}Zn_{0.25}^{2+}Al_{0.25}^{3+}(OH)_2].(CO_3^{2-})_{0.125}.H_2O$ or MgZnAl-CO_3 layered double hydroxide was used as an adsorbent in the adsorption of methyl-orange from aqueous solution in a batch adsorption. A set of analytical techniques was used to characterize the material: X-ray diffraction (XRD), Fourier Transformed Infrared Spectroscopy (FTIR), Brunauer–Emmett–Teller (BET), and Transmission Electron Microscopy (TEM). The role of different parameters, such as initial dye concentration, solution pH, adsorbent dosage, contact time, and temperature, was investigated. The adsorption kinetics were studied by pseudo-first-order, pseudo-second-order, and intraparticle diffusion models. The experimental data fit well with the pseudo-second-order kinetic model. The positive value of the changes in enthalpy (ΔH^0) and the Gibbs free energy (ΔG^0) showed that the adsorption is endothermic and spontaneous for all studied temperatures. The equilibrium adsorption data was analyzed using Langmuir's and Freundlich's isotherm models. The comparative correlation coefficient R^2 defines the fit model for the analysis of experimental data. The high correlation coefficient indicates that the Langmuir isotherm model fitted the data well. Langmuir isotherm model exhibited a maximum adsorption capacity of 869.5 mg/g for calcined and 220.26 mg/g for uncalcined layered double hydroxide. This result suggests that calcined layered double hydroxide could be a promising adsorbent for removing anionic dye in wastewater.

5.2. Results and discussion

5.2.1. X-ray diffraction of uncalcined and calcined MgZnAl-CO_3 LDH

The X-ray diffraction (XRD) pattern of MgZnAl-CO_3 LDH, calcined LDH and calcined

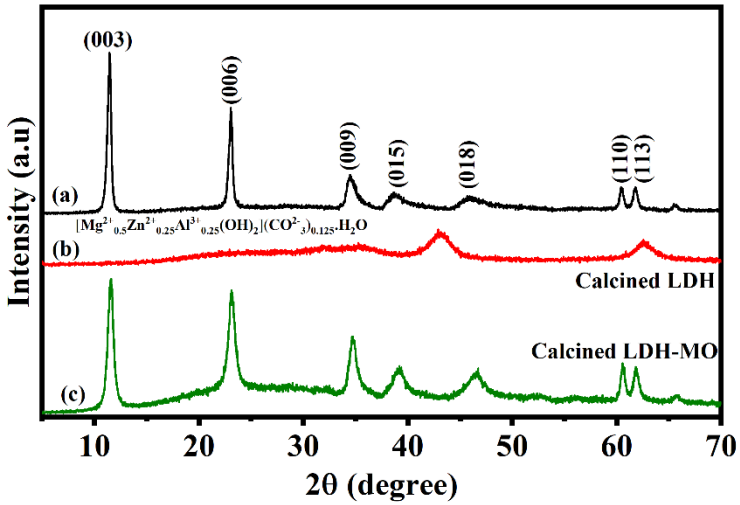

Figure 5.1: X-ray diffraction spectra of (a) MgZnAl-CO_3 (b) calcined layered double hydroxide and (c) calcined layered double hydroxide after Methyl-orange adsorption.

LDH after adsorption of methyl-orange, as shown in Figure. 5.1. In Figure. 5.1a, the series of peaks (003), (006), (009), (015), (018), (110), and (113) obtained at 11.47°, 23.04°, 34.50, 38.76°, 45.79°, 60.50° and 61.80° respectively illustrated. The results suggest that the synthesized LDH possesses a well-organized crystalline structure with distinct layers. No other phase was observed; the similar observations are cited in the literature [205–207]. The XRD pattern of calcined LDH is shown in Figure. 5.1b. This pattern indicates that the heat treatment destroyed the layered structure and converted it to an amorphous material after calcination. This implies that most interlayer anions and water molecules were removed during the process. The material was calcined at 500 °C for 4 h; after that, most of the peaks disappeared, and only two broad peaks were found. The spectrum shows the formation of metal oxide such as MgO and ZnO. There was no aluminium oxide peak because of the low calcined temperature [206]. The X-ray diffraction pattern of calcined LDH after adsorption of MO is shown in Figure. 5.1c. This spectrum shows that the initial peak position is identical but with lower intensity than layered double hydroxide. The primary mechanism behind the structure reconstruction of calcined LDH after adsorption of methyl-orange; most of the

interlayered anions are OH^- coming from MO and CO_3 is coming from air medium into the interlayer of LDH.

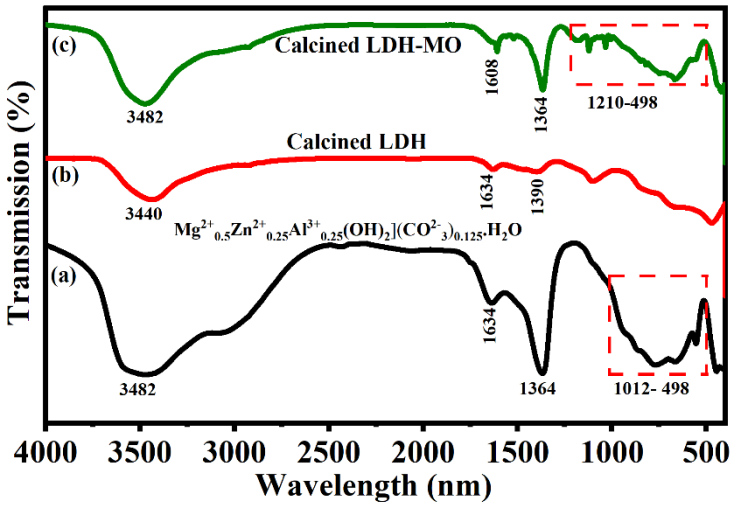

Figure 5.2: Fourier transformed infrared spectra of (a) MgZnAl-CO_3 LDH (b) calcined MgZnAl-CO_3 LDH (c) and calcined MgZnAl-CO_3 LDH after adsorption methyl-orange.

5.2.2. Fourier Transform Infrared spectrum analysis

The Fourier transform infrared (FTIR) spectrum of calcined, uncalcined, and after adsorption of MO by calcined LDH as shown in Figure. 5.2. This spectrum illustrates that the bands associated with the stretching and bending vibrations of intercalated anions within the interlayer of materials, along with the stretching vibration band of metal-oxygen-metal. The broad and significantly intense peak at 3482 cm^{-1} corresponds to the stretching vibration of the O-H bond, attributed to water molecules within the material layers. This pattern remains consistent after the adsorption of MO by calcined LDH. However, in the case of calcined LDH, there is a minor shift and a decrease in intensity compared to LDH, which can be ascribed to the elevated calcination temperature, as depicted in Figure 5.2 [208,209]. The weak band near around 1634 cm^{-1} assigned the bending vibration of water molecules (deformation mode, $\partial H-O-OH$), and intensity became less due to calcined temperature for calcined LDH. Also, a slight shift in the adsorption of MO by calcined LDH, with a peak at 1608 cm^{-1}, confirmed the material involved in Methyl-orange adsorption

[205,210]. The strong peak around 1364 cm^{-1}, both for uncalcined LDH and MO adsorbed by calcined LDH, represents the symmetric stretching of intercalated CO_3 anion between the stacked materials [211]. This peak became less intense and slightly shifted due to the high calcined temperature for calcined LDH but did not wholly vanish of intercalated anions. This finding is consistent with earlier research indicating that intercalated anions eliminate temperatures above 700 °C [210]. The band in the range of $498 - 1012\ cm^{-1}$ is assigned to the metal-oxygen-metal stretching band ($Metal = Mg, Zn, and\ Al$) [212–214]. In Figure 5.2.c, there is some change in bond length in the range of $498 - 1012\ cm^{-1}$, confirming calcined LDH involved methyl-orange adsorption (approved by the XRD spectra).

5.2.3. Nitrogen adsorption-desorption isotherm

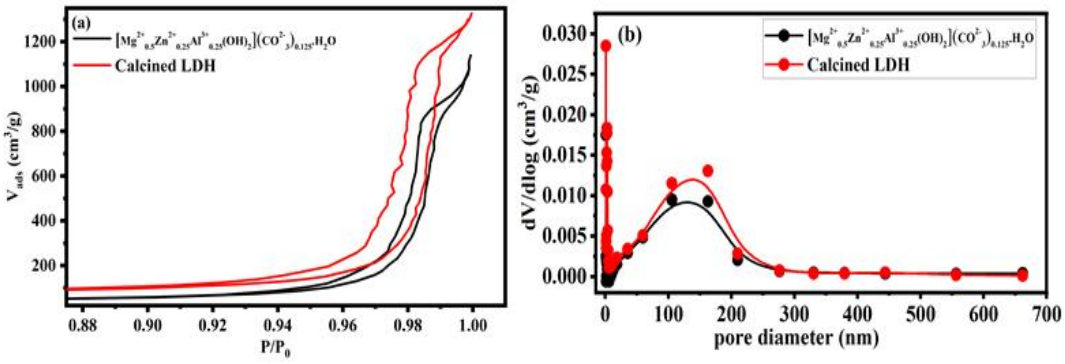

Figure 5.3: (a) Nitrogen adsorption-desorption isotherms and (b) corresponding pore size distribution curve for MgZnAl-CO_3 LDH and calcined MgZnAl-CO_3 LDH.

The nitrogen adsorption-desorption and pore size distribution curves for uncalcined and calcined LDH are shown in Figure. 5.3a and 5.3b. According to the previous study, this material exhibits type V isotherm, which is very unusual and correlated with type III isotherm according to the classification of J Zhou et al. [215]. In this case, the interaction between the adsorbent and adsorbate is fragile. In Figure. 5.3a, this isotherm exhibits an H1 type of hysteresis at high relative pressure, typically consisting of an agglomerated surface and regular array shape with uniformity and broad distribution of pore size. This type of hysteresis is typically correlated with porous materials, which quickly diffuse any reactants through these large pore sizes. The pore size distribution curve for both calcined and uncalcined materials is shown in Figure 5.3b. The nature of this curve is the same for both materials, with a broad range of up to 300 nm. This

porosity is confirmed as mesoporous and macroporous, which can be associated with the pores formed between the stacked nanosheets [216]. These materials are very suitable as adsorbents for adsorption of methyl-orange due to their inherent mesoporosity and macroporosity.

The textural properties were calculated and listed in Table 5.1. The specific surface area of the MgZnAl-CO_3 increase from 65 to 130 $^{m^2}/_{g}$ and the pore volume from 1.31 to 1.74 $^{cm^3}/_{g}$ by calcining the material at 500 °C for 4 h. The calcination temperature causes removal of water and anion molecules, ensuring the formation of channels and porous materials that may potentially increase pore volume and specific surface area.

Table 5.1: Textural properties of the sample

Sample name	Surface area ($^{m^2}/_{g}$)	Average pore diameter (nm)	Pore volume ($^{cm^3}/_{g}$)
MgZnAl-CO_3 LDH	**65**	**80.94**	**1.31**
Calcined MgZnAl-CO_3 LDH	**130**	**53.79**	**1.74**

5.2.4 Morphological analysis

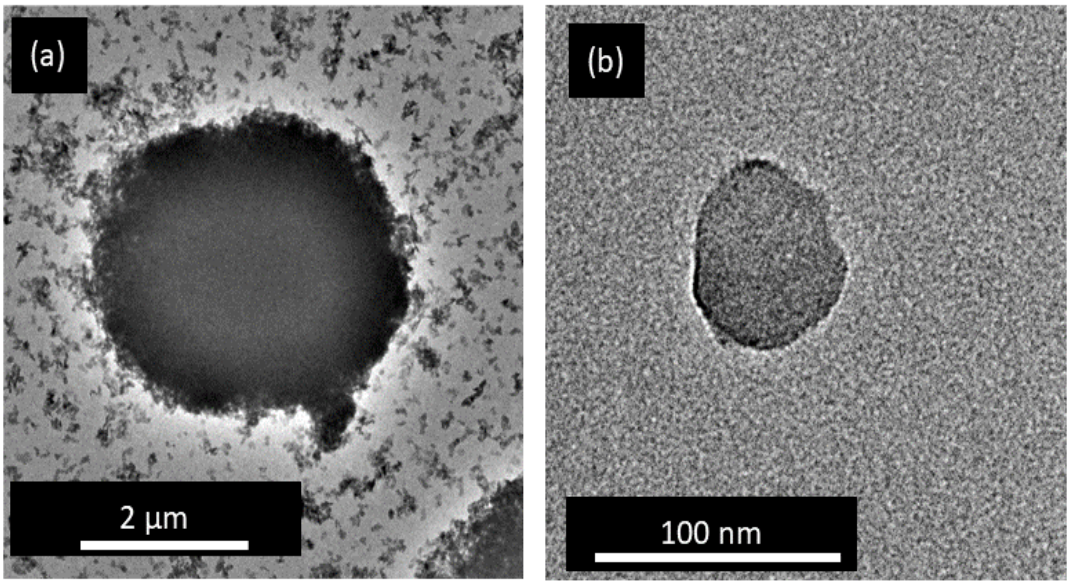

Figure 5.4: Transmission electron microscopy images of MgZnAl-CO_3 layered double hydroxide at different magnification.

The Transmission electron spectroscopy (TEM) images of prepare MgZnAl-CO_3 LDH, as shown in Figure 5.4. The higher and lower-resolution TEM images revealed that the material exhibited a well-defined hexagonal structure [217,218].

5.3. Kinetic studies

5.3.1. The effect of solution pH

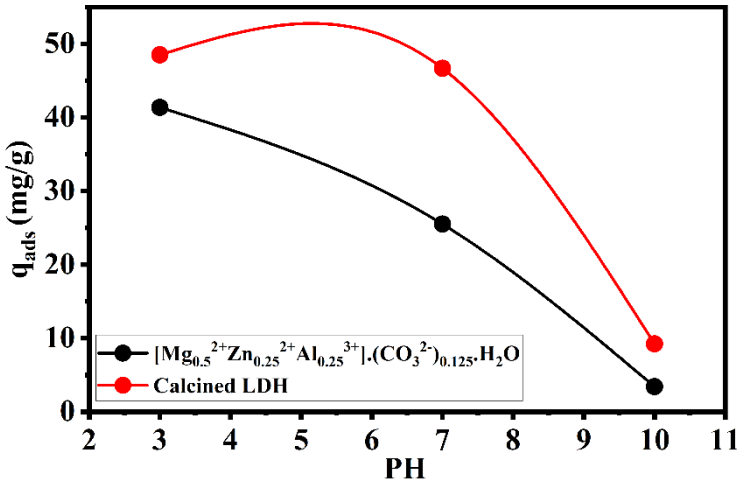

Figure 5.5: Effect of pH in adsorption of Methyl-orange on the two samples (V_{sol}=50 ml, adsorbent mass = 50 mg, C_0=50 mg/L, dots represent the q_{ads} (mg/g)**.**

The solution's pH is an important parameter in the adsorption process. The effect of pH on the adsorption of MO by the uncalcined and calcined materials is shown in Figure 5.5. The maximum adsorption capacities are 3 ± 1 to 48 ± 1 mg/g by LDH and 9 ± 1 to 46 ± 1 mg/g by calcined LDH at pH value 3 to 10 at a constant initial concentration of 50 mg/L. The uptake value of MO by the material is decreased with increased pH. At a higher pH (above 9), an increase of OH^- ions in the solution, increases the interaction competition between the OH^- and anionic species of dye, indicating a decrease in adsorption amount. The adsorption of MO was enhanced when the solution pH was below 4. MO acquires a more negative charge below pH 4 due to deprotonation reaction $(RNH^+(-CH_3)_2 \rightarrow\equiv RN(CH_3)_2 + H^+)$ and $-SO_3Na$ groups of MO being ionized and transform to $-SO_3^-$. Consequently, the rise in MO adsorption is a result of the electrostatic interactions between the positive charges of LDH and calcined LDH, and the negative charge of the MO molecules. So, the maximum adsorption capacity

was observed at pH 3 to 4, aligning with findings previously reported in the literature [219]. Based on the examination of pH influence, it can be concluded that the primary adsorption mechanism for MO adsorption is electrostatic interaction. However, all the adsorption processes were conducted at normal pH.

5.3.2. Effect of contact time on Methyl-orange adsorption

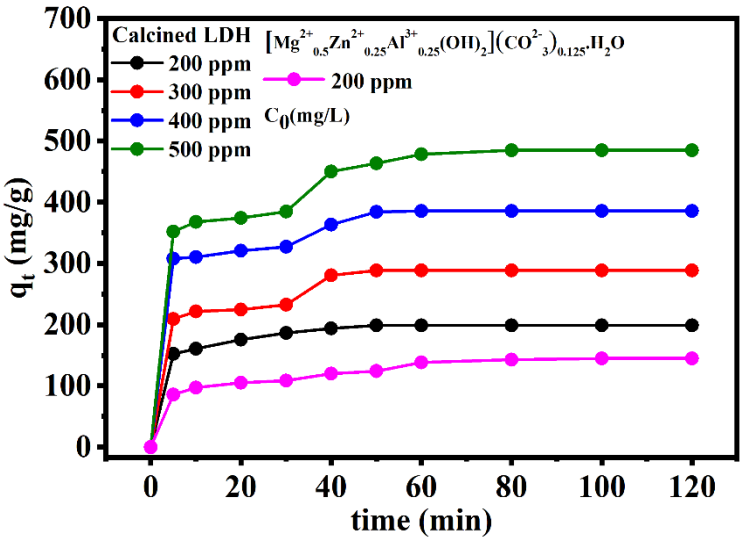

Figure 5.6: Effect of time and initial concentration in the adsorption of Methyl-orange on the two samples (V_{sol} =50 ml, adsorbent mass = 50 mg, pH=7).

One of the crucial factors in the adsorption process is the effect of contact time. The duration required for the dye to be removed from an aqueous solution is depicted in Figure 5.6. This figure shows that the amount of MO adsorbed by calcined LDH rapidly increased initially 5 to 10 minutes and once again in the range of 30 to 40 minutes for 300 to 500 ppm. After that, the process slowly increased towards the equilibrium value. At last, it became saturated after 60 minutes. For lower concentrations of MO (less than 300 ppm), equilibrium was reached early. Meanwhile, for LDH, at an initial 5 to 10 minutes, the adsorption process increased and very slowly increased with time, and after 40 minutes, it was saturated. At the same concentration (200 ppm), the equilibrium state comes at different times: 60 minutes by calcined LDH and 40 minutes by LDH. The variation in the time to reach equilibrium between LDH and calcined LDH can be

elucidated by the MO anions adhering to the surface of calcined LDH and the anion exchange process facilitated through reconstruction (Memory effect). However, the reconstruction process for high MO concentration requires time. In this instance, the MO diffuses throughout the layer of calcined materials and takes some time to reach saturation. In the case of uncalcined LDH, MO adsorbed onto the outer surface only because carbonate ions are loosely bound to the outer surface of the material and can be replaced by the anion of MO. Figure 5.6 shows that calcined LDH has higher adsorption efficiency than MgZnAl-CO_3 at the same concentration of MO.

5.3.3. Effect of methyl-orange (MO) concentration

The MO concentration impacts the materials' ability to adsorb MO. The amount of MO adsorbed by the calcined LDH increased from 197 to 484 mg/g, as shown in Table 5.2. The removal percentage of MO decreased from 98.5 % to 96.8 % with an increase in concentration of 200 to 500 mg/L. The elevated removal percentage observed at low MO concentrations can be attributed to the increased ratio between the adsorbent's active sites and MO. This facilitates greater uptake at lower concentrations. Since the number of active sites on the surface of a specific amount of adsorbent is always the same, the removal percentage decreases as the MO concentration increases.

5.3.4. Effect of adsorbent dosage

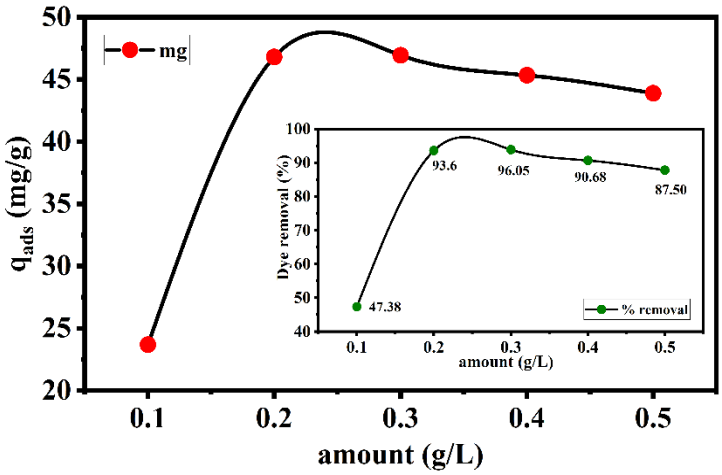

Figure 5.7: Effect of adsorbent dosage in the adsorption of Methyl-orange on calcined layered double hydroxide ($V_{sol} = 50\ ml$, $C_0 = 50\ ^{mg}/_{L}$.

The amount of adsorbent dosage can affect the removal efficiency of methyl-orange, as shown in Figure 5.7. The percentage removal of methyl-orange increased from 47.38 to 96.05 % when the adsorbent dosage rose from 0.1 to 0.3 g/L, and the removal percentage decreased from 96.05 to 87.5 % with an increase in adsorbent dosage from 0.3 to 0.5 g/L. Furthermore, the lower and higher uptake capacity of calcined LDH at fixed amounts of MO concentration, 50 mg/L removal from aqueous solution, is shown in Figure 5.7. In the case of low adsorbent dosage, LDH is easily dispersed in an aqueous solution, so all active sites present on the surface are entirely exposed, which will efficiently adsorb the MO molecules. In this instance, the surface adsorption is rapidly saturated and demonstrates a greater adsorption capacity. On the other hand, at higher adsorbent dosages, lower energy sites quickly occupy higher energy active sites, suggesting a lower uptake capacity. In addition to this factor, an increase in the collision

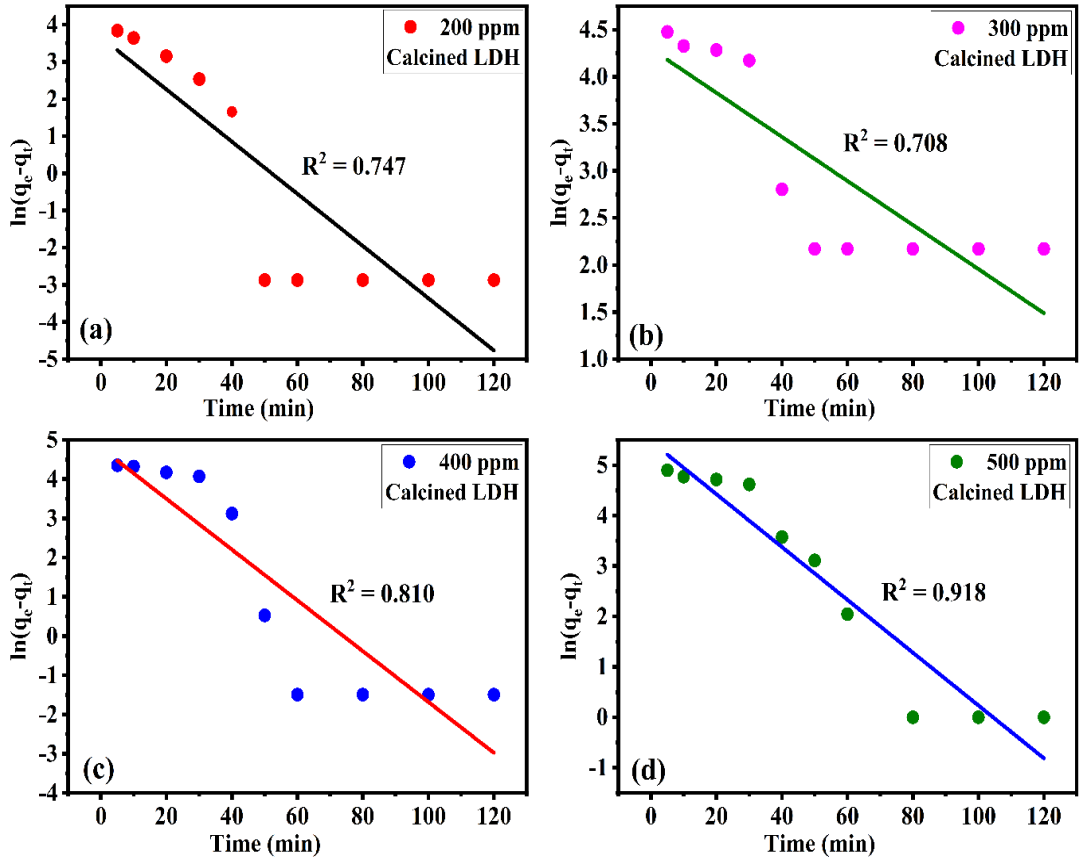

Figure 5.8: Pseudo-first-order kinetic for adsorption of Methyl-orange on calcined MgZnAl-CO_3 layered double hydroxide, dot represents the experimental data and line define linear fit (V_{sol} = 50 ml, adsorbent mass = 50 mg (which is not applicable for lower R^2).

rate between adsorbent and adsorbate molecules, an extension of the diffusion path, and a reduction in the surface area of active sites all contribute to the decline in MO's adsorption capacity.

5.4. Kinetic model applied to the adsorption of Methyl-orange onto the uncalcined and calcined MgZnAl-CO_3 layered double hydroxide

To predict the adsorption kinetics of the adsorption process, pseudo-first-order, pseudo-second-order, and intraparticle diffusion models were used to test the experimental MO adsorption data onto the uncalcined and calcined LDH. The kinetics of MO adsorption using the pseudo-first-order model can be expressed by the equation (3)

$$\ln(q_e - q_t) = lnq_e - k_1 t \ldots\ldots\ldots\ldots\ldots\ldots\ldots\ldots\ldots\ldots \quad (3)$$

The pseudo-second-order model can be expressed by the equation (4)

$$\frac{t}{q_t} = \frac{1}{k_2 q_e^2} + \frac{1}{q_e} t \ldots\ldots\ldots\ldots\ldots\ldots\ldots\ldots\ldots\ldots\ldots\ldots\ldots \quad (4)$$

The conformity test of the model predicted data and experimental data was expressed by the correlation coefficient R^2. Where the adsorption rate constant k_1, k_2 and R^2 with a correlation coefficient of pseudo-first-order and pseudo-second-order kinetic models are shown in Table 5.2. The linear form of the pseudo-first-order and pseudo-second-order kinetic models of calcined LDH is shown in Figure. 5.8 and Figure. 5.9. The rate constant of the pseudo-second-order decreased from 22.31×10^{-4} to 3.8×10^{-4} min^{-1}, and the rate constant of the pseudo-first-order decreased from -5.8 to -4.3 $min^{-1}$with increasing the Methyl-orange concentration from 200 to 500 mg/L has shown in Table 5.2. The value of q_e continuously increases with increasing the value of MO concentration. The equilibrium adsorption capacity determined using calcined LDH closely matched the calculated value derived from the fitted kinetic model. The correlation coefficient value R^2 is higher for pseudo-second-order than pseudo-first-order.

Table 5.2. Kinetic model parameters obtained in adsorption of Methyl-orange onto the calcined and uncalcined $MgZnAl-CO_3$ layered double hydroxide pseudo-second-order and pseudo-first-order.

C_0 (mg/L)	$q_{e,exp}$ (mg/g)	Pseudo-second-order			Pseudo-first-order		
		$q_{e,cal}$ (mg/g)	k_1 (10^{-4})	R^2	$q_{e,cal}$	$k_1(10^{-4})$	R^2
Calcined layered double hydroxide							
200	197	203	22.31	0.999	38	-5.8	0.747
300	297	301	7.8	0.996	73	-1.9	0.708
400	392	398	7.5	0.998	120	-5.3	0.810
500	484	507	3.8	0.997	237	-4.3	0.918
MgZnAl LDH							
200	154	155	7.5	0.994	171	-5.2	0.909

C_0 (mg/L), q_e (mg/g), $k_1(min^{-1})$, $k_2(g\ (mg.\ min)^{-1})$

These results indicate that a pseudo-second-order model fits the experimental data and is suitable for discussing MO adsorption onto the calcined LDH. The pseudo-second-

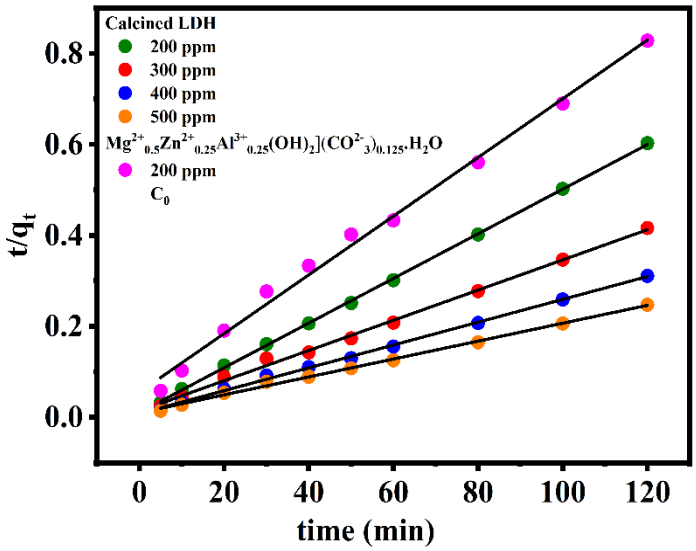

Figure 5.9: Pseudo-second-order kinetic for adsorption of Methyl-orange on the two samples (V_{sol}= 50 ml, adsorbent mass = 50 mg, (ppm=mg/L), dot represents the experimental value, line indicates the linear fitting.

order model is consistent with a chemisorption mechanism as the rate-determining step and is based on the adsorption loading on the solid phase. The pseudo-second-order model also has the benefit of being able to predict behaviour across the entire range of the adsorption process.

The intraparticle diffusion model discovered by Weber and Morris is used to discuss the diffusion mechanism in the adsorption of MO onto the calcined LDH in equation (5)

$$q_t = k_i t^{1/2} + C \ldots\ldots\ldots\ldots\ldots\ldots (5)$$

In this equation (5), $k_i\left(mg/gmin^{-1/2}\right)$ is the intraparticle diffusion rate constant and $C(mg/g)$ is the intercept of this equation. The plot of $q_t\ vs\ t^{1/2}$ is shown in Figure 5.10. The intraparticle diffusion model proposes a potential mechanism for adsorption, illustrating how it occurs as a function of time within the particle. Due to the porous nature of particle textures, the adsorption process can take place in multiple ways and involve distinct stages, including external mass transfer, internal diffusion of adsorbate into the adsorbent, and adsorption onto active sites on the surface. The intraparticle diffusion model shows three different regions for Methyl-orange concentrations of 300 to 500 mg/L, which are attributed to external surface instantaneous adsorption (K_{D1}), gradual intraparticle diffusion (K_{D2}) and final equilibrium stage (K_{D3}), where the available active sites are decreased, and intraparticle diffusion slows down. The first

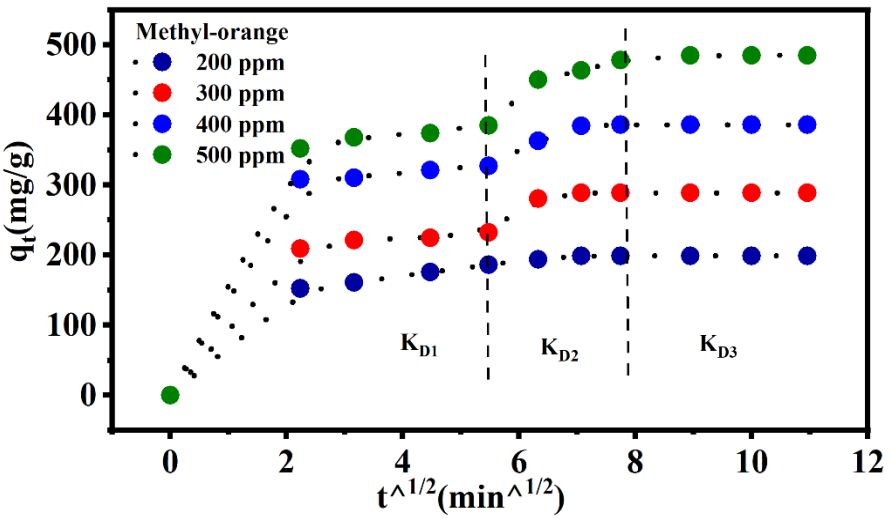

Figure 5.10: Intraparticle diffusion model for calcination layered double hydroxide (ppm=mg/L), dot represents the experimental data**.**

step shows a higher adsorption rate in the first 30 minutes. The second step is related to the rate-determining step; in this step, intraparticle diffusion occurs. The last step is also associated with the rate-determined step, but adsorption becomes saturated with the gradual saturation of adsorption sites at this stage. For less concentration of methyl-orange (200 ppm), the profile of the adsorption process occurred in a single step. This feature indicates that adsorption occurs on the external surface of the material with low concentrations of methyl-orange [220].

5.5. Adsorption thermodynamic

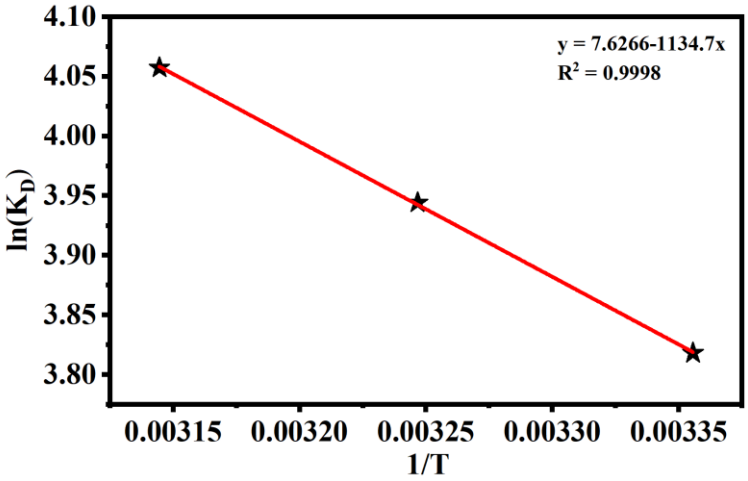

Figure 5.11: Van't Hoff plot for the adsorption of methyl-orange dye on calcined layered double hydroxide, red line indicates the linear fit and star sign is experimental value.

Thermodynamic parameters like Gibbs free energy change ΔG^0, standard enthalpy change ΔH^0, and standard entropy change ΔS^0 were also studied to understand how temperature affects the adsorption. Experimental was conducted using a 100 mg/L concentration of MO solution (50 ml) and 50 mg of adsorbent, at different temperatures of 25, 35 and 45 ± 1 °C. The following equation calculated the thermodynamic parameters ΔG^0, ΔH^0 and ΔS^0

$$lnK_D = \frac{\Delta S^0}{R} - \frac{\Delta H^0}{RT} \quad \ldots\ldots\ldots\ldots (6)$$

$$\text{And } K_D = \frac{q_e}{C_e} \quad \ldots\ldots\ldots\ldots\ldots\ldots (7)$$

Where R is the ideal constant, T is the temperature (K), and K_D is the distribution coefficient. The plot of lnK_D vs $\frac{1}{T}$ gives the straight line (Figure. 5.11), slope and intercept corresponding to the $\frac{\Delta H^0}{R}$ and $\frac{\Delta S^0}{R}$, respectively. The values of ΔG^0 were calculated at different temperatures used in the experiment using the following equation:

$$\Delta G^0 = \Delta H^0 - T\Delta S^0 \text{ .... (8)}$$

The results are displayed in Table 5.3; the negative value of the ΔG^0at different temperatures indicates the adsorption's feasibility and the spontaneous nature. The negative value of the ΔG^0 increases with the temperature increase, which shows that the adsorption process is more spontaneous at high temperatures. The positive value of ΔH^0 (9.4 KJ/mol) indicates that the adsorption process is endothermic and physical. The positive value ΔS^0 of the system calcined LDH-MO adsorption suggests an increase of the randomness at the interface of adsorbent/adsorbate during the adsorption process.

Table 5.3: Values of the thermodynamic parameters for adsorption of Methyl-orange on calcined layered double hydroxide.

Temperature (K)	$\Delta G^0 \left(\frac{KJ}{mol}\right)$	$\Delta H^0 \left(\frac{KJ}{mol}\right)$	$\Delta S^0 \left(\frac{J}{mol\ K}\right)$
298	-9.45		
308	-10	9.4	63.37
318	-10.71		

5.6. Adsorption isotherm

In the solid-liquid system, the adsorption equilibrium is one of the most important to define how much adsorbate is adsorbed by the adsorbent. Batch experiments at different adsorbate concentrations clarified the phenomena of adsorption isotherm. Langmuir and Freundlich, two well-known models, are suitable for discussing this work. The numerous factors obtained from the two models explain the adsorption mechanism, surface behaviours and the affinity between adsorbate and adsorbent. The Langmuir isotherm model predicts that the energy of the adsorption process is constant, and a

certain number of active sites are constantly available on the surface of the adsorbate; a single monolayer occupies each site. It is described by the equation

$$\frac{1}{q_e} = \frac{1}{(q_m \times K_L \times C_e)} + \frac{1}{q_m} \ldots\ldots\ldots\ldots\ldots\ldots\ldots\ldots (9)$$

or $$\frac{C_e}{q_e} = \frac{1}{(K_L \times q_m)} + \frac{C_e}{q_m}$$

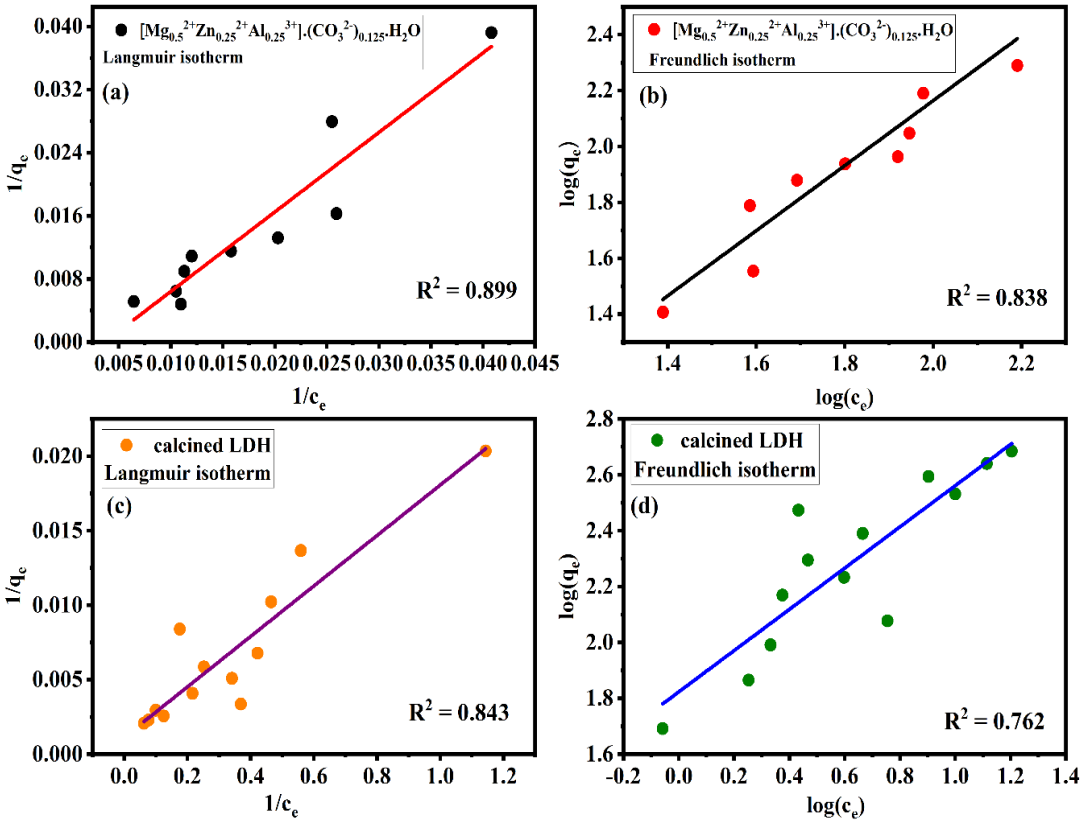

Figure 5.12: Langmuir and Freundlich isotherm model of Methyl-orange adsorption by $MgZnAl - CO_3$ (a & b) and by calcined layered double hydroxide (c & d), dot represents the experimental value and line indicate the fitting (R^2 of Langmuir isotherm is greater than Freundlich isotherm, so Langmuir is applicable here).

The maximum adsorption (q_m) value is evaluated from the Langmuir isotherm model, correlating to the whole monolayer coverage on the adsorbent surface. The adsorption isotherm model of MO is adsorbed by the uncalcined, and calcined LDH, as shown in Figure 5.12. The liner plot of $\frac{1}{C_e}$ vs $\frac{1}{q_e}$ gives the maximum adsorption capacity (q_m) value and the Langmuir constant related to the adsorption energy. This value of q_m calculated from these isotherm models confirmed that MO adsorbed by the calcined LDH is higher than MgZnAl LDH. The surface charge of LDH is positive, and the

surface charge of MO is negative, so the main reason behind the adsorption process is the coulomb attraction force between the adsorbate and adsorbent.

Table 5.4 shows the result of the linear plot of the Langmuir and Freundlich isotherm model. Both models' correlation coefficient value R^2 confirmed the suitable isotherm model to discuss. Here, the value R^2 of the Langmuir isotherm model is greater than the Freundlich model, indicating the homogeneous adsorption process and formation of a monolayer of MO onto the calcined LDH surface. The maximum adsorption capacity of MO by the calcined LDH is more significant than uncalcined LDH. The amount of MO was adsorbed 869.56 mg/g and 220.26 mg/g by the calcined and uncalcined LDH, similar adsorbate adsorbed by different materials, is listed in Table 5.5. This difference in adsorption capacity will increase the surface area as well as porosity during the calcination process of the material. The Freundlich isotherm model predicted that the surface of materials becomes heterogeneous during the adsorption process. The Freundlich isotherm model constant K_f and n provides the adsorption process's approximated adsorption capacity and intensity. The Freundlich isotherm model was described by the equation (10).

$$\log(q_e) = \log(K_f) + \frac{1}{n}\log(C_e) \; or \; q_e = K_f C_e^{\frac{1}{n}} \quad \text{(10)}$$

The curve was plotted against $logq_e \; vs \; logC_e$ gives the values of K_f and n. K_f related to the bonding energy represents the quantity adsorbed by the adsorbent surface per equilibrium concentration and defines the adsorption coefficient or distribution coefficient. The value of $\frac{1}{n}$ indicates the adsorption intensities of adsorbent or surface heterogeneity, which becomes more heterogeneity if the value of $\frac{1}{n}$ becomes close to zero. The value $\frac{1}{n}$ is greater than 1, which indicates cooperative adsorption, and less than 1 indicates the normal Langmuir isotherm.

Table 5.4. Langmuir and Freundlich isotherm model constant and correlation coefficient for methyl-orange adsorption onto the calcined and uncalcined layered double hydroxide.

Isotherm model	MgZnAl-CO_3 LDH	Calcined layered double hydroxide
Langmuir Isotherm	$q_m = 220.26\ mg/g$ $K_L = 0.0114\ L/mg$ R^2 =0.899	$q_m = 869.56\ mg/g$ K_L =0.068 L/mg R^2 =0.838
Freundlich Isotherm	$K_f = 3.133\ mg/g$ n = 1.209 $\frac{1}{n} = 0.827$ $R^2 = 0.843$	K_f =66.374 mg/g n =1.355 $\frac{1}{n}$ =0.738 R^2= 0.762

Table 5.5. Comparison of monolayer equilibrium adsorption capacity for Methyl-orange adsorption with other adsorbents.

Adsorbent	$q_m(\frac{mg}{g})$	References
Calcined MgZnAl $-$ CO_3 layered double hydroxide	**869.56**	**This Work**
MgNiAl $-$ C	375	[221]
GO $-$ LDH	505.1	[222]
Fe $-$ Mg	370.36	[223]
Glycerol-modified layered double hydroxide	1062.3	[219]
RGO modified Ni-Cr	312.5	[224]
CTMAB/10SST-MMT	149.25	[225]
Calcined Lapindo Volcanic mud	333.3	[226]

5.7. Economical analysis

The cost analysis of the wastewater treatment and adsorbent preparation demonstrates the financial feasibility of the adsorbent. The entire cost analysis is performed based on

lab scale, but only chemical purchases can be found using the industrial cost basis and supplies from the India Mart location. The material preparation cost is based on the price of energy and chemicals purchased. The energy cost for the material preparation is determined by taking into account the cost of Indian electricity used for the synthesis process, sample heating, drying and purchasing costs of $Mg(NO_3)_2$, $Zn(NO_3)_2$, $Al(NO_3)_3$, NaOH, and Na_2CO_3. The estimated cost is calculated for removing the Methyl-orange from the aqueous solution.

In this section, we solely calculated the estimated adsorption expenses necessary to treat each litre (L) of wastewater containing, 100 mg/L concentration. The calculation was based on one-time adsorption and desorption of MO from the wastewater by the calcined LDH. The cost required for the wastewater treatment and comparison to other methods is shown in Tables 5.6 and 5.7. Our cost analysis used a lab basis, but the industrial basis calculation will be significantly cheaper than the lab basis calculation. The required adsorption cost by calcined LDH is 0.09 Indian rupees per Litter wastewater. Applying calcined LDH for wastewater treatment containing MO can save adsorption costs compared to other methods and adsorbents.

The high adsorption capacity and low preparation cost of calcined LDH support its potential as an effective and low-cost adsorbent for removing wastewater containing methyl-orange pollutants.

Table 5.6: Cost analysis for calcined layered double hydroxide for wastewater treatment.

Material Name	Average Adsorption Capacity (mg/g)	Preparation cost (Rs) (for 500gm)	Adsorption cost (Rs/L)
Calcined $MgZnAl-CO_3$ layered double hydroxide	**869.56**	**382**	**0.09**

Table 5.7: Effective cost analysis of wastewater treatment with different techniques.

Methods	Operating Cost (US$)
Adsorption Method using calcined MgZnAl-CO_3 layered double hydroxide	**0.001/L (This Work)**
Electro Coagulation	0.47/L[227]
Chemical Coagulation	0.2/L[227]
Fenton Oxidation	0.026-0.046/L[228]
Photo-Fenton Oxidation	0.027-0.036/L[228]

5.8. Adsorption Mechanism

In dye adsorption, the significant contributing interactions typically include electrostatic forces, ion exchange, surface area, hydrogen bonding, and metal coordination. Based on this, the high adsorption capacity of the calcined LDH may be considered more than the interaction mentioned above. The surface charge of the LDH is positive, and MO has a negative surface charge that may initiate the electrostatic interaction and play a significant role in the adsorption process. At the same time, other interactions are also responsible for the adsorption process. The high surface area of the calcined LDH (130 $^{m^2}/_{g}$) is another reason for the high adsorption capacity of the adsorbate. In this study, the calcined LDH demonstrates an outstanding adsorption capacity for the anionic dye methyl-orange. This dye has a sulphonyl group (SO_3^{2-}) responsible for electrostatic interaction with a positive surface charge of the LDH [229]. On the other hand, MO contains only the opposing group and an azo group ($-N = N-$) which is its only mechanism for forming metal coordination. The adsorption mechanism involves four regions: (1) the initial rise in adsorption rate occurs due to the electrostatic interactions, external surface charge and hydrogen bonding, $n - \pi$ and $\pi - \pi$ interaction are therefore responsible for MO uptake and metal coordination between the surface charge of the solid and the molecules being adsorbed, as verified by the Langmuir adsorption isotherm, indicating the formation of a monolayer (2) in this

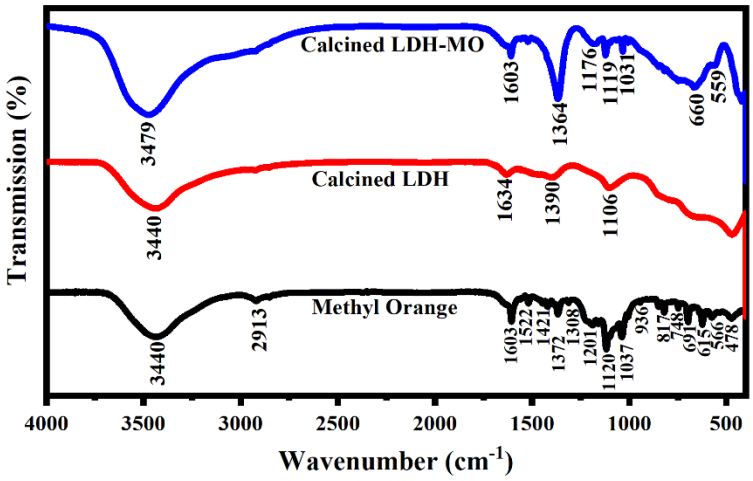

Figure 5.13: Fourier transform infrared spectroscopy spectra of methyl-orange, calcined MgZnAl-CO_3 LDH, and after methyl-orange adsorption on calcined MgZnAl-CO_3 LDH.

region, the adsorption process continues happening due to the isoelectric point appears and the interaction initiated between adsorbent molecules and high concentration of dyes, (3) with increased concentrations of the adsorbate; there is a notable occurrence of second-layer adsorption. In this phase, individual adsorbed adsorbate molecules act as an active site, leading to the formation of hemimicelles and a remarkable enhancement in the adsorption rate, (4) above the critical micelle concentration, the surface is covered mainly with hemimicelles, leading to no further measurable change in the adsorption capacity [230,231].To confirm the interactions, FTIR analysis of MO and calcined LDH was performed after and before MO adsorption, as shown in Figure 5.13. In the case of MO, the peaks at 1120 cm^{-1} and 1037 cm^{-1}arise from the sulphonic group and slightly shift to 1119 cm^{-1} and 1031 cm^{-1},after adsorption [230]. The formation of complexes might suggest the presence of metal on the calcined LDH surface, where the metal interacts with oxygen through unidentate bonding. The high surface charge of the LDH indicates that electrostatic interaction contributes a primary role to the adsorption process at the adsorbent.

5.9. Conclusion

The outcomes of this investigation have proposed that the ternary LDH exhibits high efficiency in removing methyl-orange from wastewater. The calcined layered double hydroxide has shown higher removal efficiency of methyl-orange than MgZnAl-CO_3 layered double hydroxide. The pseudo-second-order model suitably fitted kinetic data of the adsorption process, while the Langmuir isotherm model represented the

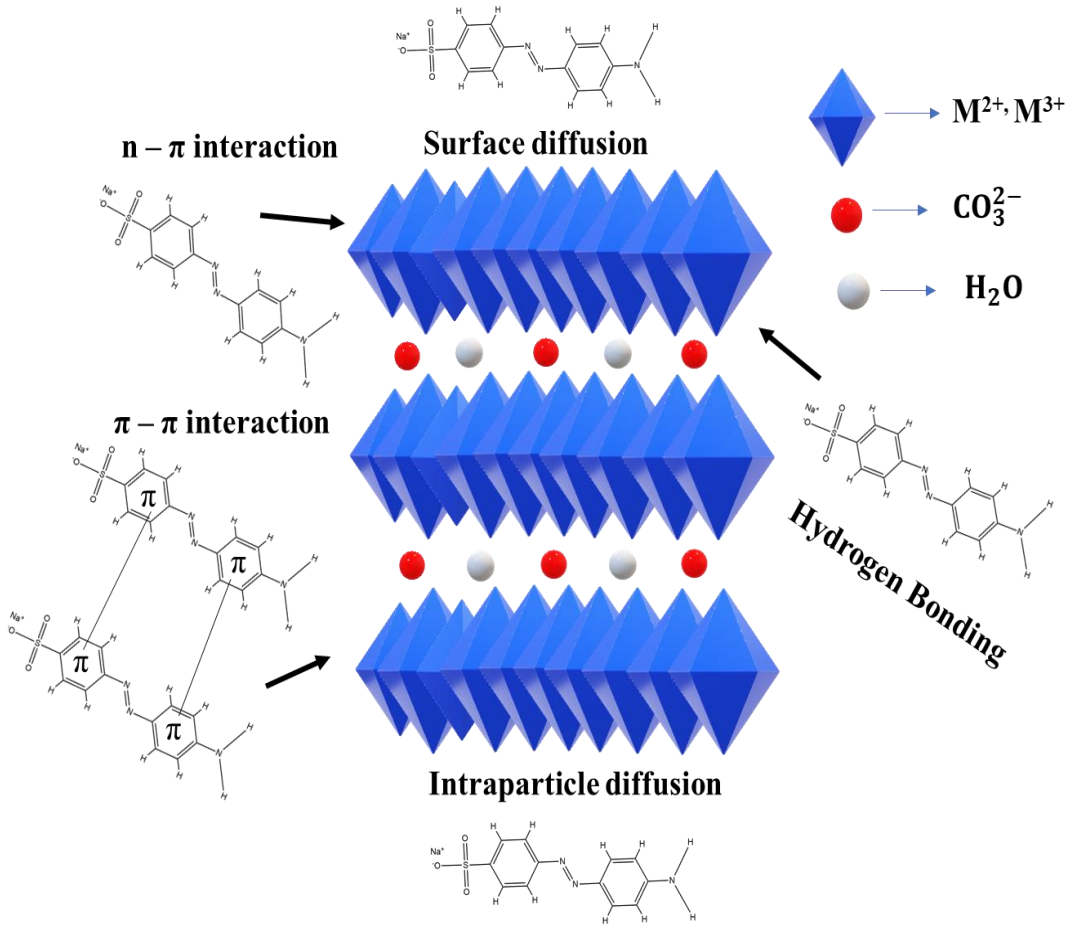

Figure 5.14: Schematic diagram of MO adsorption.

adsorption isotherm data. The prepared ternary layered double hydroxide was designed and fabricated to remove Methyl-orange with high concentration and an equilibrium adsorption time of less than 40 min. The thermodynamic constant was also evaluated using an equilibrium equation with changing the temperature. A negative value of ΔG^0 at the different temperatures indicated spontaneity, and the positive value of ΔH^0 showed the endothermic nature of the adsorption process. The maximum adsorption capacity was 869.56 mg/g and 220.26 mg/g by the calcined and uncalcined layered double hydroxide. Our material is very competitive compared to other adsorbents (shown in Table 5.5).

Interestingly, the adsorption mechanism is demonstrated with the help of Fourier's transform infrared spectroscopy analysis. From this, it can be inferred that the initial stage of the adsorption process involves electrostatic interactions. The second step is forming a hemi-micelles interaction between the dye and material surface. The outcome adsorption value of the material is a promising adsorbent for removing the methyl-orange from industrial wastewater.